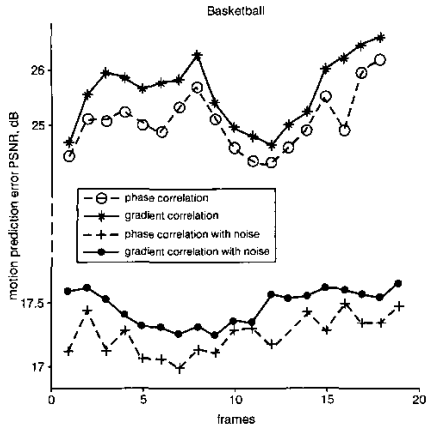

Fig. 4 *PSNR against frame number for local (block-based) motion compensated prediction in presence of noise*

Next, local motion was estimated using 32×32 pixel blocks. Results shown in Figs. 3 and 4 confirm the efficiency of gradient correlation. Table 1 ('Local') shows average MSE values obtained for the entire sequences.

Finally, additive Gaussian noise was manually induced. Figs. 3 and 4 show the PSNR of the motion compensated prediction error for noise power of 18 dB, confirming that our scheme is consistently more immune to noise. Experiments with other levels of noise power demonstrated that similar performance gains are achievable.

Conclusions: A gradient-based scheme suitable for the sub-pixel estimation of motion in video sequences is presented. The scheme yields very accurate sub-pixel motion estimates for a variety of test material and motion scenarios, including manually induced additive Gaussian noise, and outperforms phase correlation, which is among the methods of choice for professional studio applications. One of the most attractive features of the proposed scheme is a high degree of computational efficiency because it can be implemented by fast transformation algorithms in the frequency domain.

13 May 2003
Electronics Letters Online No: 20030666
DOI: 10.1049/el:20030666

V. Argyriou and T. Vlachos (*School of Electronics and Physical Sciences, Centre for Vision, Speech and Signal Processing, University of Surrey, GU2 7XH, United Kingdom*)

References

1 PEARSON, J.J., *et al.*: 'Video rate image correlation processor', *Proc. SPIE*, **119**, pp. 197–205, Applications of Digital Image Processing, 1977
2 THOMAS, G.A.: 'Television motion measurement for DATV and other applications', *BBC Res. Dept. Rep.*, No. 1987/11
3 MANDUCHI, R., and MIAN, G.A.: 'Accuracy analysis for correlation-based image registration algorithms'. Proc. IEEE-ISCAS, Chicago, IL, USA, May 1993, pp. 834–837
4 FOROOSH, H., ZERUBIA, J., and BERTHOD, M.: 'Extension of phase correlation to sub-pixel registration', *IEEE Trans. Image Process.*, 2002, **11**, (3), pp. 188–200
5 BARNEA, D.I., and SILVERMAN, H.F.: 'A class of algorithms for fast digital image registration', *IEEE Trans. Comput.*, 1972, **C-21**, (2), pp. 179–186
6 ANDRUS, J.F., CAMPBELL, C.W., and JAYROE, R.R.: 'Digital image registration method using boundary maps', *IEEE Trans. Comput.*, 1975, **C-24**, (9), pp. 935–940
7 BEAUCHEMIN, S.S., and BARRON, J.L.: 'The computation of optical flow', *ACM Comput. Surv.*, 1996, **27**, (3), pp. 433–467
8 MORANDI, C., PIAZZA, F., and CAPANCIONI, R.: 'Digital image registration by phase correlation between boundary maps', *IEE Proc. E*, 1987, **134**, (2), pp. 101–104
9 FITCH, A.J., *et al.*: 'Orientation correlation'. Proc. British Machine Vision Conference, 2002, Vol. 1, pp. 133–142
10 CHRISTMAS, W.J.: 'Spatial filtering requirements for gradient-based optical flow measurement', *IEEE Trans. Image Process.*, 2000, **9**, (10), pp. 1817–1820

Thick-film PZT-metallic triple beam resonator

T. Yan, B.E. Jones, R.T. Rakowski, M.J. Tudor, S.P. Beeby and N.M. White

A metallic triple-beam resonator with thick-film piezoelectric elements to drive and detect vibrations is presented. The resonator substrate was fabricated by a double-sided photochemical-etching technique and the thick-film piezoelectric elements were deposited by a standard screen-printing process. The resonator, 15.5 mm long and 7 mm wide, has a favoured mode at 6.2 kHz with a Q-factor of 3100.

Introduction: The thick film printing process has been successfully used to deposit piezoelectric materials onto silicon structures for fabrication of a silicon beam resonator and other silicon devices [1]. In this Letter we describe the application of this process to the fabrication of a metallic triple beam resonator with screen-printed thick-film lead zirconate titanate (PZT) drive and sense elements and present initial results from the device. This device, a metallic triple beam tuning fork structure with thick-film printed piezoelectric drive and pickup elements, is the first of its kind [2].

Resonator design and fabrication: The resonator consists of three beams (tines) aligned in parallel alongside each other and joined at a decoupling zone at each end which is in turn connected to the surrounding material. The central beam is twice the width of the two outer beams. The resonating element has a length of 15.5 mm, a thickness of 0.25 mm and beam widths of 2 and 1 mm. The distance between the beams is 0.5 mm. Finite element analysis (FEA) has been performed to predict the modal behaviour with stress distribution and eigenfrequencies of the resonator. Thick-film PZT elements were printed on separate regions at each end of the central beam, where maximum stresses exist as the resonator operates in its favoured mode of vibration. The PZT element at one end drives the vibrations, whilst the PZT element on the other end detects them. Positioning the PZT driving and sensing elements on the regions of maximum stresses maximises the degree of mechanical coupling between the active piezoelectric layer and the resonator for generation of both driving forces and sensing signals.

The triple beam resonator has three different fundamental modes of vibration out of the plane of the wafer. In mode one, the three tines oscillate in phase. In mode two, the central tine does not oscillate while the outer tines vibrate at a phase of 180° with respect to each other. In mode three, the central tine vibrates in anti-phase with the outer tines. This mode is the optimum for operating such a triple beam resonator, as both bending moments and shearing forces at the decoupling zone are cancelled out and very little vibration energy is coupled into the supporting frame at each end. This improves the Q-factor of the device and therefore the performance of a resonant sensor employing such a device. The in-phase mode has the lowest resonant frequency, followed by the second and third modes. There are also other higher-order modes of vibrations. A photograph of the metallic resonator is shown in Fig. 1.

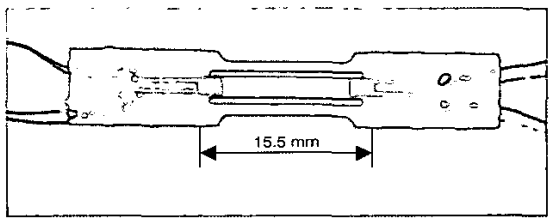

Fig. 1 *Photograph of metallic resonator*

The substrate of the resonator was fabricated from a 0.5 mm-thick 430S17 stainless steel thin wafer using a simultaneous double-sided photochemical etching technique, with a top pattern to define the layout of the resonator and a bottom pattern to etch in a standoff distance leaving the section of resonating element 0.25 mm thick. A dielectric layer was then deposited at the defined driving and sensing regions on the top surface of the resonator using a standard screen-printing process, and consecutively layers of bottom gold electrode, piezoelectric paste

and top gold electrode, were deposited each with their own screens. The dielectric layer was required to isolate the bottom electrode from the resonator substrate in order to polarise the piezoelectric layer in a later stage.

The fabricated resonators were sawn from the wafer and electrical connections were made by conventional wire bonding. The PZT elements were then connected in parallel and poled for 1 h at 130°C with a voltage of 200 V across the electrodes. Given the measured PZT layer thickness of 50 μm, an electric field of strength 4 MV/m was generated during the polarising process. This aligns the dipoles within the PZT material enabling it to exhibit its piezoelectric properties.

Resonator operation and results: The resonator operating in air was first tested in an open-loop configuration in order to observe the vibration modes and confirm successful operation of the driving and sensing mechanisms. The PZT element at one end of the resonator was driven by an AC signal of 1 V peak-peak from a Hewlett-Packard 89410A vector signal analyser with the tracking generator scanning over a frequency range of 2–9 kHz. The PZT element on the other end of the resonator was connected to a Kistler 5011 charge amplifier and the output from the charge amplifier was fed back to the signal analyser for frequency response analysis of the resonator. Fig. 2 shows the frequency response of the resonator with clear resonances at 2.2, 6.2 and 6.8 kHz. These resonances correspond to the first, the third and the fourth vibration modes of the resonator respectively, according to the FEA predictions, with the third mode of vibration being far dominant due to the favourable dynamic structure balance associated with this mode. It is clear that the peak corresponding to mode two is not visible, since in this mode the central beam, where the pick-up is located, is at rest.

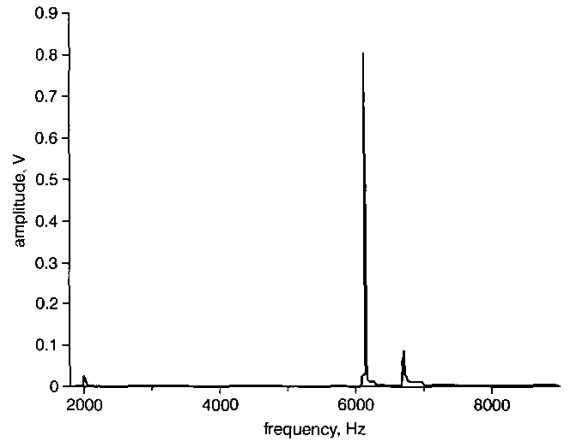

Fig. 2 *Amplitude–frequency response of resonator*

The Q-factor of the resonator in air for mode three was measured to be 3100, which is excellent when compared to a Q-factor 70 of a silicon single beam resonator with PZT thick films operating in air [1] or a Q-factor 400 of a silicon triple beam resonator with thin films vibrating in air [3] or the Q-factors of other metallic resonators [4] in air.

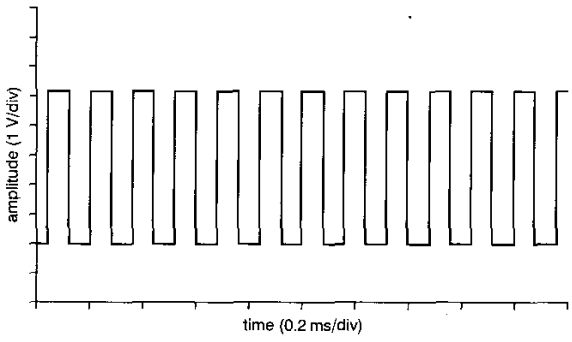

Fig. 3 *Frequency output of resonator in closed-loop*

Next, the resonator (in air) was tested in a feedback closed-loop configuration. The PZT sensing element was connected to a charge amplifier circuit, followed by a digital 90° phase shift circuit and a second stage amplification circuit all on one circuit board. The output from the second stage amplification was fed back to the other PZT element for driving. In such a way, the resonator was maintained at resonance in the required favourable mode of oscillation. Fig. 3 shows the frequency output of the resonator in such a closed-loop operation.

Conclusions: This Letter has reported for the first time a metallic triple beam resonator etched from stainless steel in which the vibrations are driven and detected by thick-film printed piezoelectric elements. The resonator has been characterised in an open-loop test which identified the modes of vibration and confirmed the successful operation of the device and of the driving and sensing mechanisms. The resonator has further successfully been operated in a closed-loop configuration with the designed associated electronics. The presented resonator has shown a good mode selectivity with a Q-factor of 3100 operating in air, which compares very favourably with other reported resonators of similar structures operating in air. This device can be easily mass-produced at low cost for use in a wide range of measuring systems, e.g. load cells, weighing machines, torque transducers and pressure sensors. Details of characteristics, interfacing and other sizes/material configurations are under investigation.

Acknowledgments: The authors wish to acknowledge the support of EPSRC (Grant GR/R51773) and the industrial collaborators within the Intersect Intelligent Sensing Faraday Partnership Flagship Project (2002–2005) entitled 'Resonant Microsensor Modules for Measurement of Physical Quantities (REMISE)'.

28 April 2003
Electronics Letters Online No: 20030611
DOI: 10.1049/el:20030611

T. Yan, B.E. Jones and R.T. Rakowski (*The Brunel Centre for Manufacturing Metrology, Brunel University, Uxbridge, Middlesex UB8 3PH, United Kingdom*)

E-mail: barry.jones@brunel.ac.uk

M.J. Tudor, S.P. Beeby and N.M. White (*Department of Electronics and Computer Science, University of Southampton, Highfield, Southampton, Hampshire SO17 1BJ, United Kingdom*)

References

1 BEEBY, S.P., and WHITE, N.M.: 'Thick-film PZT – silicon micromachined resonator', *Electron. Lett.*, 2000, **36**, (19), pp. 1661–1662
2 JONES, B.E., and WHITE, N.M.: 'Metallic resonators'. Patent Application GB0302585.5, 2003
3 FABULA, T.H., WAGNER, H.-J., and SCHMIDT, B.: 'Triple-beam resonant force sensor based on piezoelectric thin films', *Sens. Actuators A*, 1994, **41–42**, pp. 375–380
4 RANDALL, D.S., RUDKIN, M.J., CHESHMEHDOOST, A., and JONES, B.E.: 'A pressure transducer using a metallic triple-beam tuning fork', *Sens. Actuators A*, 1997, **60**, pp. 160–162

High performance 10–12.5 Gbit/s modulator driver in InP SHBT technology

Zhihao Lao, M. Yu, V. Ho, K. Guinn, Muliang Xu, Shing Lee, V. Radisic and K.C. Wang

A high performance modulator driver circuit is presented using 4″ InP SHBT technology. The IC was developed for driving EAM modulators in OC-192 (10 Gbit/s) and with forward error correction (FEC: 10.7 Gbit/s or 12.5 Gbit/s) optical fibre systems. The monolithic integrated circuit features output amplitude control, output crossing point control and output DC offset control. Measured results show the circuit operates at 10 to 12.5 Gbit/s with a swing of 3.1 V_{p-p} at each output and 20/18 ps rise/fall times. The power dissipation is 1.4 W with a standard power supply of −5.2 V.